# Overlayer Strain Relief on Surfaces with Square Symmetry: Phase Diagram for a 2D Frenkel-Kontorova Model

J.C. Hamilton
*Sandia National Laboratory, Livermore, California 94550*

(Received 5 November 2001; published 11 March 2002)

Overlayers on surfaces with square symmetry exhibit a huge variety of strain relief mechanisms. I present a simple 2D Frenkel-Kontorova model and calculate the associated zero temperature phase diagram which shows a transition from overlayers with square symmetry (and possible square dislocation patterns) to hexagonal symmetry. The phase diagram includes the experimentally observed clock-rotated phase. Local density approximation calculations suggested by the model show that a clean Ni(100) surface reconstructs from a bulk-terminated to a clock-rotated structure at biaxial compressive strains above 2.5%.

DOI: 10.1103/PhysRevLett.88.126101 PACS numbers: 68.35.Bs, 68.35.Md, 68.55.Jk

Virtually every surface, with or without a heteroepitaxial overlayer, is strained. For clean surfaces, the coordination of surface atoms is lower than bulk atoms, thus the surface atoms prefer a different interatomic spacing from the bulk atoms. For overlayers, the lattice constants of the overlayer and the substrate are not perfectly matched. Since the mechanisms of strain relief determine the structure of clean surfaces and overlayers, it is essential to understand these mechanisms in order to predict and control such structures.

In this paper, I consider the structure of overlayers on surfaces with square symmetry. Experimentally a great variety of structures has been observed for overlayers on (100) surfaces. These include pseudomorphic structures, pseudomorphic structures with intersecting rectangular dislocation arrays [1], clock-rotated structures [2], hexagonal overlayers of various periodicities [3], and rotated hexagonal overlayers [4]. More recently, nonintersecting dislocation lines have been observed for Cu deposited on Ni(100) [5]. Ideally, one would have a single theory which can explain in a systematic manner the wide range of structures observed for overlayer systems on (100) surfaces. This has proved an elusive goal.

There are a number of theoretical approaches that have been applied to this problem. The classic work in this area is by Frank and van der Merwe (FVM) [6]. In their continuum approach they consider the problem as two superimposed one-dimensional problems. Their theory predicts intersecting dislocations forming an approximately square grid. It has been extremely successful in addressing issues of strained layer growth on Si(100), for example. Their theory cannot, however, treat situations in which a hexagonal film forms on a square substrate. Other work has addressed the reconstruction of fcc metal 100 surfaces, specifically Au, Pt, and Ir to form hexagonal overlayers, sometimes rotated with respect to the substrate [7]. Finally, there is considerable work using molecular dynamics [8] and/or Monte Carlo techniques [9] to study the structure of films grown on (100) surfaces.

In this paper I consider the phase diagram for a model of an overlayer on a square substrate as a function of the lattice mismatch between substrate and overlayer. The most important feature of this model is that it includes both hexagonal and square symmetry overlayers and the transition between these two symmetries. In contrast to molecular dynamics and Monte Carlo techniques, the energetics of defect free single phases at 0 K are calculated and compared. This 2D Frenkel Kontorova (FK) model is of fundamental theoretical interest. In addition, the solutions are useful because they suggest phases which should be tested in detailed atomistic calculations of strain relief. As an example of this application, first-principles calculations performed here show that a nickel (100) surface subjected to a strain parallel to the surface reconstructs from a bulk termination to a clock rotation for biaxial compressive strain exceeding 2.4%.

For a 2D Frenkel Kontorova model the adatoms move in a substrate potential:

$$V_{\mathrm{sub}}(\vec{\mathrm{r}}) = \frac{V_0}{4}\left(\cos\frac{2\pi x}{a} + \cos\frac{2\pi y}{a} + 2\right).$$

$V_0$ determines the strength of the substrate potential and $a$ is the lattice constant for the 2D square surface lattice. For the numerical study reported here, $V_0$ was chosen as 0.8 eV corresponding to a fourfold hollow energy of 0.0 eV, a bridge site energy of 0.4 eV, and an on-top site energy of 0.8 eV. These are plausible values for a (100) fcc metal surface. The lattice spacing $a$ was set equal to 2.49 Å, the nearest neighbor spacing of bulk nickel.

In a 1D Frenkel-Kontorova model, nearest neighbor atoms are connected by springs. Since the atoms are in a linear chain, each atom has one nearest neighbor on each side. In a 2D Frenkel-Kontorova model, the definition of nearest neighbors can be problematic, and it is customary to avoid ambiguity by using a short range adatom-adatom potential with a binding energy, $\varepsilon$. Lennard-Jones and Morse potentials are common choices. In order to facilitate comparison with analytical calculations, including the work of FVM, I chose instead a piecewise continuous function made of two parabolic segments. This potential is shown in Fig. 1. Over most of its range ($r < r_1$) it has the form $V(r) = -\varepsilon + (k/2)(r - r_0)^2$. The minimum of this potential is at $r = r_0$ and the binding energy is $\varepsilon$. In order to continue this function to zero, it was joined to an inverted parabola for the remainder of its range, $V(r) = -(k/2)(r - r_2)^2$ for $(r_1 < r < r_2)$. By matching $V(r)$ and its derivative at $r_1$, the values of $r_1$ and $r_2$ are determined. The range of the potential is $r_2 = r_0 + 2\sqrt{\varepsilon/k}$.

The value for $\varepsilon$ was initially chosen to fit the cohesive energy of nickel and the value of $k$ was chosen based on a Lennard-Jones potential with the binding energy and lattice constant of nickel. This choice ($\varepsilon = 0.7$ eV and $k = 10$ eV/Å$^2$) gave hexagonal overlayers for all values of the overlayer misfit. In order to investigate the competition between pseudomorphic and hexagonal overlayers commonly seen for metal surfaces and overlayers, I chose instead $\varepsilon = 0.35$ eV and $k = 10$ eV/Å$^2$. All of the results reported here were obtained with these parameters.

The total energy of a system of adatoms adsorbed on the surface is the sum of the substrate energy for all of the adatoms, and the adatom energy for all of the adatom-adatom bonds:

$$E_{\text{total}} = \sum_j V_{\text{sub}}(\vec{r}_j) + \sum_{i \neq j} \sum_j V_{\text{ad}}(|\vec{r}_i - \vec{r}_j|)/2\,.$$

The energy per atom, $E$, is this energy divided by the number of adatoms. In order to construct the zero temperature phase diagram for this model, one must find single phase arrangements of atoms which fill two-dimensional space (with periodic boundary conditions) and which minimize $E$. I started with a variety of initial atomic configurations (to be described), picked a value of the lattice mismatch, $\Delta = (r_0 - a)/a$, and used the conjugate gradient technique to minimize the total energy as a function of the atomic positions. The calculations were limited to mismatches in the range $-0.2 < \Delta < 0.2$. Atomic arrangements resulting from the minimization with more than one phase or with defects were rejected. By repeating this procedure for a complete set of reasonable initial trial configurations, the global minimum energy configuration was found for various values of the mismatch, $\Delta$. In practice, the key issue was to identify a complete set of reasonable initial trial configurations. It was hard to be sure that this set was complete. I was guided in this task by experimental results showing configurations with fourfold coordination to other adatoms (rectangular packing) and configurations with sixfold coordination to other adatoms (hexagonal packing). These configurations were placed on the substrate with periodic boundary conditions and dimension $40a$ by $40a$.

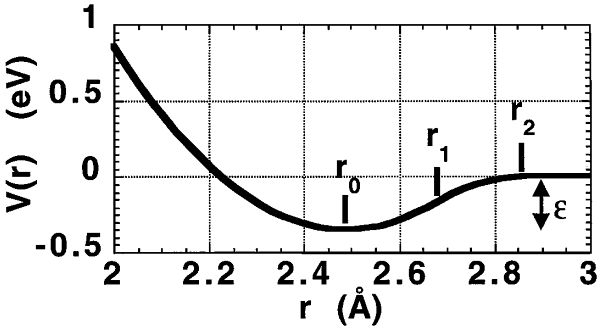

FIG. 1. Adatom-adatom potential used in these calculations. The potential has a binding energy, $\varepsilon$, a spring constant, $k$, and is parabolic for $r < r_1$. For $r > r_1$ the potential is an inverted parabola, out to a cutoff radius at $r_2$.

We first consider phases generated starting with rectangular packing. The initial configurations were generated using lattice vectors $\vec{b} = (40a/n)\hat{x}$ and $\vec{c} = (40a/m)\hat{y}$, where $\hat{x}$ and $\hat{y}$ are unit vectors in the $x$ and $y$ directions. Most of the phases generated starting with rectangular packing correspond to the phases predicted by FVM [6]. For $n = m < 40$, a square dislocation array with light-wall dislocations is formed (see Fig. 2a). For $n = m > 40$, a square dislocation array with heavy-wall dislocations is formed. In agreement with the FVM solution, the lowest energy solutions are square dislocation arrays ($n = m$). For $n = m = 40$, a pseudomorphic phase with all of the adatoms in fourfold hollow sites can be produced. However, the ability to simultaneously relax atomic coordinates in two dimensions allows another strain relief mechanism which is not possible in the FVM theory. This "clock-rotated" phase, shown in Fig. 2b, has been seen experimentally for various adsorbates on (100) surfaces. For our parameters it was stable for adatom bond lengths in the range between about $1.02a$ and $1.08a$.

We next consider phases generated starting with hexagonal packing. The initial configurations were generated using lattice vectors $\vec{b} = (40a/n)\hat{x}$ and $\vec{c} = (20a/n)\hat{x} + (40a/m)\hat{y}$, where $\hat{x}$ and $\hat{y}$ are unit vectors in the $x$ and $y$ directions, respectively. This choice of lattice vectors allows the approximately hexagonal array to fit perfectly on the square substrate. The extent to which the arrays are

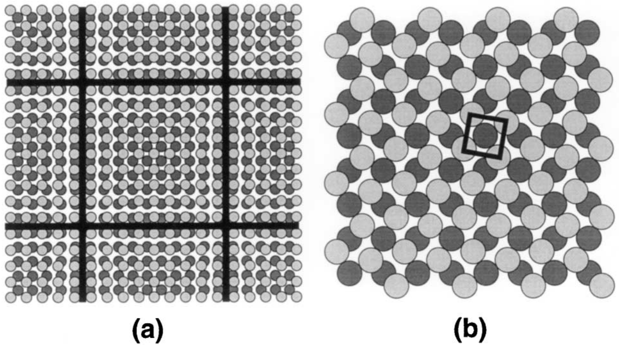
(a) (b)

FIG. 2. Typical structures formed by minimizing the energy of initial structures with rectangular packing. (a) The square dislocation pattern predicted by Frank and van der Merwe. The dislocations are indicated by the heavy lines. (b) The clock rotation. Units of four adatoms are rotated clockwise and expanded slightly relative to the pseudomorphic structure. This increases the length of the bonds within the unit of four atoms. It also brings some atoms within a neighboring unit closer.

distorted from perfect hexagonal packing is determined by the choice of $n$ and $m$. (An approximately hexagonal array would have $m \approx 2\sqrt{3}\,n/3$.) For positive mismatch, phases with $m = 40$ were favored (see Fig. 3a). I will call these phases registered. For these registered phases all the adatoms lie along parallel lines (horizontal in Fig. 3a) containing fourfold hollow and bridge sites. All of the adatoms avoid on-top sites, and are at least a distance of $a/2$ from the on-top sites. This strong registry to the substrate allows strain relief while avoiding the energetically costly on-top sites. For negative mismatch, phases with $m > 40$ were favored, some adatoms were near on-top sites, and the phase was called unregistered (see Fig. 3b).

Phases generated with hexagonal packing rotated by small angles relative to the substrate were also considered. The energies of the rotated overlayers were very slightly larger than the energies of unrotated overlayers shown in Fig. 3. This is in accord with the theoretical predictions from an analytical FK model treating only hexagonal layers [10]. As discussed in Ref. [10], it appears that rotated overlayers can be explained only in a 2D FK model by allowing higher order terms in the substrate potential.

Once the energy per atom, $E$, has been calculated as a function of the misfit, $\Delta$, it is straightforward to determine the zero temperature phase diagram by plotting $E$ vs $\Delta$ for the various phases. Because there are so many possible phases, these data are presented in two different plots in Fig. 4. The upper plot includes only the pseudomorphic and square dislocation phases. Since this plot includes only those phases allowed in the continuum theory of FVM, its predictions agree with that theory. The structure is pseudomorphic for $|\Delta| < 0.075$. For larger misfits, square arrays of dislocations form with dislocation spacing decreasing as the misfit increases in agreement with FVM.

In the lower plot of Fig. 4, $E$ vs $\Delta$ is plotted for the unregistered hexagonal, pseudomorphic, clock-rotated, and registered hexagonal phases. Comparison with the upper plot shows clearly that the clock-rotated and hexagonal phases are lower in energy than square arrays of dislocations over the whole misfit range. The model predicts unregistered hexagonal phases for $-0.2 < \Delta < -0.025$, the pseudomorphic phase for $-0.025 < \Delta < 0.025$, the clock-rotated phase for $0.025 < \Delta < 0.085$, and registered hexagonal phases for $0.085 < \Delta < 0.2$.

The phase diagram will, of course, depend upon the values chosen for the model parameters. Since the driving force for formation of hexagonal layers is the increase in the adatom-adatom coordination, a fourfold coordinated structure is favored for smaller values of the adatom-adatom binding energy, $\varepsilon$, whereas a sixfold coordinated structure is favored for larger values of $\varepsilon$. The main effect of varying the adatom-adatom potential was found to be shifting the relative energies of the fourfold coordinated and sixfold coordinated structures. Experimentally, metal on metal systems tend to show pseudomorphic, clock, and hexagonal structures. I chose the adatom-adatom potential to favor this range of structures.

This model provides a simple and mathematically attractive model of strain relief. There are a number of experimental systems which exhibit phases identical to those

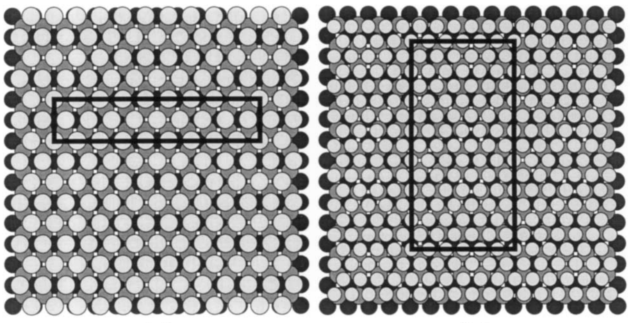
(a) (b)

FIG. 3. Typical structures formed by minimizing the energy of initial structures with hexagonal packing. (a) A hexagonal structure formed when the overlayer atoms are larger than the substrate atoms ($\Delta = +0.12$). This structure is called registered because the rows of adatoms remain over the fourfold hollow and bridge sites of the substrate. (b) A hexagonal structure formed when the overlayer atoms are smaller than the substrate atoms (here $\Delta = -0.16$). The structure shown in (b) will be called unregistered because some of the adatoms lie near on-top sites.

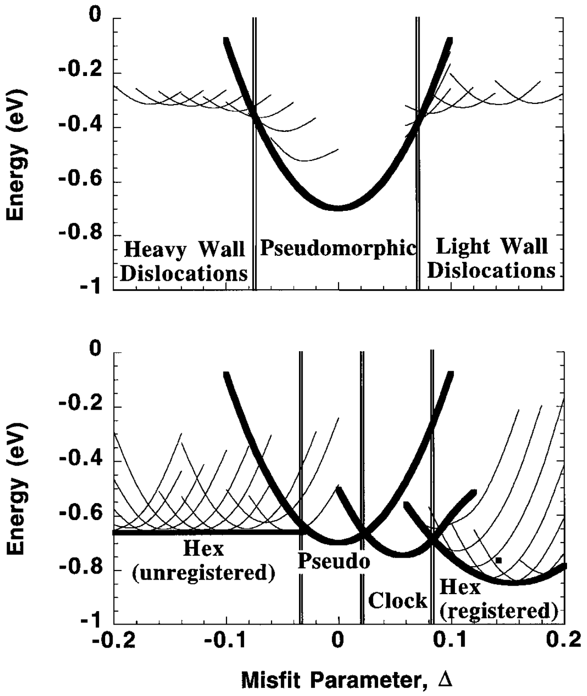

FIG. 4. Plot of energy vs misfit parameter for various possible structures. The upper plot shows only the phases permitted by the FVM model, i.e., pseudomorphic and square dislocation arrays. The lower plot shows the phases which actually have the lowest energy for this model, i.e., unregistered hexagonal, pseudomorphic, clock-rotated, and registered hexagonal. For the registered hexagonal, the phases plotted as light parabolas have $n = 40$, and $m = 39$ (not stable), 38, 37, 36, 35, 34, and 33, respectively. The $n = 40$, $m = 36$ phase is identical to the $c(10 \times 2)$ reconstruction seen for Ag on Cu(100).

predicted by this model. Clean Pt(100), Au(100), and Ir(100) surfaces all exhibit unregistered hexagonal reconstructions [11]. Ni(100) surfaces form a clock-rotated phase upon absorption of one half a monolayer of carbon [2] or nitrogen [12]. Silver atoms absorbed on Ni(100) or Cu(100) exhibit registered hexagonal overlayers with $c(2 \times 8)$ and $c(2 \times 10)$ structures, respectively, in excellent agreement with this model [13].

The simple model presented here is intended as a qualitative theory for overlayer strain relief. However, it can also be very useful in suggesting structures likely to be found experimentally or in highly accurate first-principles calculations. For example, one might suspect based on this model that a clock-rotated surface structure should be formed on an fcc (100) metal surface if the bulk sample is subjected to a biaxial compressive strain parallel to the surface. This would be expected because the compressive strain would reduce the bulk lattice constant in the directions parallel to the surface. Thus the effective misfit, $\Delta$, between the surface atoms and the bulk would become positive. I have checked this prediction using the first-principles ultrasoft pseudopotential code, VASP. The initial system was a five-layer Ni slab with two free (100) surfaces. The total number of atoms in the unit cell was 20. The energy cutoff was 242 eV and there were 3 $k$ points in the irreducible Brillouin zone. The energy difference between the pseudomorphic and clock-rotated phase changed by 60 meV upon increasing to 10 k points in the irreducible zone. I conclude that the calculations were adequately converged, since this change does not affect the conclusion drawn from this calculation. Figure 5 shows the total energy of the 20 atom system for the pseudomorphic and the clock-rotated phases plotted as a function of the biaxial compressive strain. This calculation indicates that a nickel (100) surface will reconstruct to the clock-rotated phase for compressive strains exceeding 2.5%. This quantitative LDA calculation is in agreement with the qualitative behavior predicted by the simple 2D FK model. However, the quantitative agreement in the strain at which surface reconstruction occurs is totally fortuitous, depending upon the choice of parameters in the FK model. The success of the model in predicting this previously unexpected reconstruction under biaxial strain suggests that it will be useful in predicting other previously unobserved strain relief phenomena for overlayers on square substrates.

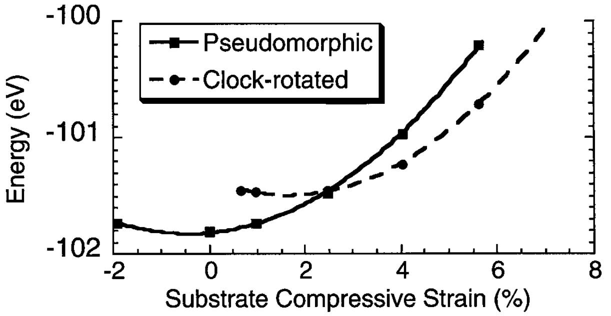

FIG. 5. First-principles local density approximation calculation for total energy of five-layer nickel slab subjected to biaxial compressive strain. As the substrate is compressed, the effective misfit between the bulk atoms with their strained lattice constant and the surface layers increases. At about 2.5% strain, the surface layer reconstructs to a clock-rotated structure.

The 2D Frenkel-Kontorova models have previously been used with great success to model overlayer structures on surfaces with hexagonal symmetry [14]. Strain relief mechanisms for surfaces with square symmetry are quite different from hexagonal surfaces, yet we see here that the 2D Frenkel-Kontorova model provides a suitable model for many of the observed overlayer reconstructions. Parameters for Frenkel-Kontorova models can be derived from first-principles calculations providing an important method of simulating overlayer structures in cases where the unit cell is much too large for complete first-principles calculations.

This work was supported by the Office of Basic Energy Science, Division of Materials Science, of the U.S. Department of Energy, under Contract No. DE-AC04-94AL85000.

---

[1] Y. Fukuda, Y. Kohama, M. Seki, and Y. Ohmachi, Jpn. J. Appl. Phys. **27**, 1593 (1988).
[2] C. Klink, L. Olesen, F. Besenbacher, I. Stensgaard, E. Laegsgaard, and N. D. Lang, Phys. Rev. Lett. **71**, 4350 (1993).
[3] J. E. Black, D. L. Mills, W. Daum, C. Stuhlmann, and H. Ibach, Surf. Sci. **217**, 529 (1989).
[4] S. G. J. Mochrie, D. M. Zehner, B. M. Ocko, and Doon Gibbs, Phys. Rev. Lett. **64**, 2925 (1990).
[5] B. Müller, B. Fischer, L. Nedelmann, A. Fricke, and K. Kern, Phys. Rev. Lett. **76**, 2358 (1996).
[6] F. C. Frank and J. H. van der Merwe, Philos. Mag. **198A**, 216 (1949).
[7] B. Dodson, Phys. Rev. Lett. **60**, 2288 (1988); N. Takeuchi, C. T. Chan, and K. M. Ho, Phys. Rev. Lett. **63**, 1273 (1989); X. Wang, Phys. Rev. Lett. **67**, 3547 (1991); V. Fiorentini, M. Methfessel, and M. Scheffler, Phys. Rev. Lett. **71**, 1051 (1993).
[8] J. A. Sprague and C. M. Gilmore, Surf. Coat. Technol. **65**, 71 (1994).
[9] A. Patrykiejew, S. Sokolowski, and K. Binder, J. Chem. Phys. **115**, 983 (2001).
[10] Y. Okwamoto and K. H. Benneman, Surf. Sci. **179**, 231 (1987).
[11] M. A. Van Hove, R. J. Koestner, P. C. Stair, J. P. Biberian, L. L. Kesmodel, I. Bartos, and G. A. Somorjai, Surf. Sci. **103**, 189 (1981).
[12] F. M. Leibsle, Surf. Sci. **297**, 98 (1993).
[13] A. Brodde, G. Wilhelmi, D. Badt, H. Wengelnik, and H. Neddermeyer, J. Vac. Sci. Technol. **9**, 920 (1991); P. T. Springer, E. Laegsgaard, and F. Besenbacher, Phys. Rev. B **54**, 8163 (1996).
[14] S. Narasimhan and D. Vanderbilt, Phys. Rev. Lett. **69**, 1564 (1993); J. C. Hamilton and S. M. Foiles, Phys. Rev. Lett. **75**, 882 (1995).